Available online at www.sciencedirect.com
ScienceDirect
Journal of Organometallic Chemistry 691 (2006) 5867–5872
Journal of Organometallic Chemistry
www.elsevier.com/locate/jorganchem

Uncommon assembling of organotellurium iodides: Synthesis and X-ray characterization of $[mesTeI(\mu\text{-}I)_2(TeImes)_2]_n$, $(C_5H_6N)_4[mesTeI_2]_2(I_3)_2$ and $\{(C_5H_6N)_3[(mesTeI_3)(\mu\text{-}I^-)(TeI_3mes)](I_3)_2\}_n$ (mes = 2,4,6-trimethylphenyl)

Eliandro Faoro, Gelson Manzoni de Oliveira *, Ernesto Schulz Lang *

LMI, Departamento de Química, Universidade Federal de Santa Maria, 97105–900 Santa Maria, RS, Brazil

Received 31 July 2006; received in revised form 21 September 2006; accepted 21 September 2006
Available online 29 September 2006

Abstract

$(MesTe)_2$ (mes = 2,4,6-trimethylphenyl) reacts with iodine in the presence of KI to give $[mesTeI(\mu\text{-}I)_2(TeImes)_2]_n$ (**1**). If pyridinium iodide and two or five equivalents of I_2 are added to the mixture $(mesTe)_2$/iodine, then $(C_5H_6N)_4[mesTeI_2]_2(I_3)_2$ (**2**) and $\{(C_5H_6N)_3[(mesTeI_3)(\mu\text{-}I^-)(TeI_3mes)](I_3)_2\}_n$ (**3**) are produced in good yields. Compounds **1**, **2** and **3** are atypical structured organotellurium iodides, attaining interionic $I_3^- \cdots I\text{–}Te^-$, $N^+\text{–}H\cdots I\text{–}Te^-$ and $N^+\text{–}H\cdots I_3^-$ secondary interactions. Complex **2** form single dimers, **1** and **3** assemble onedimensional, polymeric chains. In the neutral compound **1** tellurium occurs in the oxidation states +2 and +4. Besides the occurrence of charge transfer (CT) systems associated to the I_3^- ions, the charge delocalization in compound **3** suggests further the existence of an inner CT system within the iodine atoms I(3), I(4) and I(5).

Keywords: Organotellurium iodides; Mixed valence complexes of tellurium; Polymeric organotellurium iodides

1. Introduction

Recently we have described the preparation of the new T-shaped organotellurium(II) dihalides (PyH)[$mesTeI_2$], (PyH)[mesTeIBr] and (PyH)[mesTeICl] (Py = pyridine), starting from $(mesTe)_2$ and inserting two different halogen atoms on tellurium [1]. The anions $[mesTeI_2]^-$ and $[mesTeIBr]^-$ are assembled as dimers by reciprocal, secondary Te···X interactions, linked also to the pyridinium cations through μ-NH···X bonding; the anion $[mesTeICl]^-$ do not interact with neighboring anionic moieties, but attains also secondary NH···Cl bonding. Te···π-aryl interactions have not been detected, differently of earlier reported organochalcogen halides of tellurium[II][2]. The synthesis and the X-ray characterization of the series (PyH)[$mesTeBr_2$], (PyH)[mesTeClBr] and (PyH)[$mesTeCl_2$] were also further reported [3], but these compounds do not reproduce the assembling of the above mentioned parent dihalides, e. g., there is no dimeric association of the anions. Nevertheless, the secondary NH···X bonds of the anionic moieties toward the pyridinium cations are also evident. Both compound series have in common the fact that they have been prepared by addition of the stoichiometric amounts of pyridinium halides (PyH)X ($X = Cl^-$, Br^-, I^-) to the respective intermediary mesTeX (X = Cl, Br, I), last obtained by direct reaction of $(mesTe)_2$ with chlorine, bromine and resublimate iodine.

Since the chemistry of organochalcogen halides – particularly that of organotellurium iodides – becomes more and more interesting and attractive, we have developed new experimental routes to reach compounds with innovative architectural designs and, possibly, also with pharmacological applications. It is well known that compounds of tellurium have been abundantly explored in the medicine as

* Corresponding authors. Tel.: +55 55 3220 8757; fax: +55 55 3220 8031 (G.M. de Oliveira).
E-mail address: manzoni@quimica.ufsm.br (G.M. de Oliveira).

0022-328X/$ - see front matter © 2006 Elsevier B.V. All rights reserved.
doi:10.1016/j.jorganchem.2006.09.047

drugs for a wide range of diseases [4–6]; on the other side, iodine-125 and iodine-131 are very important in the radiotherapy, as well as radioactive tracers in diagnostic techniques of nuclear medicine [7].

If the reaction milieu – in the synthesis of the two series of compounds described in the begin of this report – is anyway disturbed by using appropriated reagents, the final products can be essentially different, structurally as well as chemically. We report now on the effects of these controlled "disturbances" on the intermediary **mesTeI** and the structural characterization of the new organotellurium iodides $[mesTeI(\mu\text{-}I)_2(TeImes)_2]_n$ (mes = mesityl) (**1**), $(C_5H_6N)_4[mesTeI_2]_2$ $(I_3)_2$ (**2**) and $\{(C_5H_6N)_3[(mesTeI_3)(\mu\text{-}I^-)(TeI_3mes)](I_3)_2\}_n$ (**3**). All the three complexes show unusual compositions and configurations: **2** (Te^{II}) and **3** (Te^{IV}) attain secondary, interanionic $I_3^- \cdots I\text{–}Te^-$ bonds and $N^+\text{–}H\cdots I\text{–}Te^-$ interactions; $N^+\text{–}H\cdots I_3^-$ contacts are present only in **3**. Complex **2** form single dimers, but **1** and **3** assemble onedimensional, polymeric chains. The neutral complex $[mesTeI(\mu\text{-}I)_2(TeImes)_2]_n$ (**1**) represents one specific example of organochalcogen halides with the chalcogen atoms presenting mixed valence states – Te^{II} and Te^{IV} – in the same molecule.

2. Experimental

All manipulations were conducted under argon by use of standard Schlenk techniques. The solvents were dried (toluene with sodium/benzophenone, CH_2Cl_2 with $CaCl_2$) and distilled before use.

2.1. $[mesTeI(\mu\text{-}I)_2(TeImes)_2]_n$ (1)

To a solution of $(mesTe)_2$ (0.148 g, 0.3 mmol) in 5 ml of toluene, 0.077 g (0.3 mmol) of resublimated iodine were added. The color of the solution turned blue (formation of the intermediary mesTeI). To this mixture KI (0.050 g, 0.3 mmol) was added as seed crystal (the alternative addition of 0.3 mmol of CsI or CsCl do not change the end results). After 5 h stirring the solution was concentrated and allowed to recrystallize at −18 °C.

Properties: air stable, cubic blue crystals. $C_{27}H_{33}I_5Te_3$ (1374.83). Yield: 90.0% based on $(mesTe)_2$; Melting point: 159.9–161.2 °C. C, H, N-analysis, Found: C, 23.49; H, 2.55; N, 0.00. Calc.: C, 23.59; H, 2.42; N, 0.00%.

IR (KBr): 2961.8 [ν(C–H)$_{ar}$], 2908.8 [ν(C–H)$_{me}$], 1588.2 [ν(C=C)], 1436.1 [δ(C–C–H)], 848.6 cm^{-1} [$\delta_{out\ pl.}$ (C–C–H)$_{mes.}$].

2.2. $(C_5H_6N)_4[mes\ TeI_2]_2(I_3)_2$ (2), $\{(C_5H_6N)_3[(mesTeI_3)(\mu\text{-}I^-)(TeI_3mes)](I_3)_2\}_n$(3)

To a solution of $(mesTe)_2$ (0.148 g, 0.3 mmol) in 5 ml of toluene, 0.077 g (0.3 mmol) of resublimated iodine were added. The color of the solution turned immediately blue. After addition of pyridinium iodide (0.096 g, 0.6 mmol) the system was stirred for 2 h and a red precipitate of (PyH)-$[mesTeI_2]$ [1] was formed. At this point the addition of two and five equivalents of I_2 (0.6 and 1.5 mmol) leads to the formation of **2** and **3**, respectively. After 1/2 h stirring the products (red precipitates) were filtered and dissolved in CH_2Cl_2. Monocrystals of **2** and **3** were obtained by recrystallization in CH_2Cl_2 at −18 °C.

$(C_5H_6N)_4[mesTeI_2]_2(I_3)_2$ (**2**): hygroscopic, rectangular black crystals. $C_{19}H_{23}I_5N_2Te$ (1041.49). Yield: 90.0% based on $(mesTe)_2$; Melting point: 152.8–154.2 °C. C, H, N-analysis, Found: C, 21.54; H, 2.46; N, 2.89. Calc.: C, 21.91; H, 2.23; N, 2.69%.

IR (KBr): 3198.5, 3142.3 [ν(N–H)], 3052.5 [ν(C–H)$_{ar}$], 2961.8 [ν(C–H)$_{me}$], 1626.5 [ν(C=C)], 1593.6 [ν(C=N)], 1522.9 [δ(C–C–H)], 1475.0 [δ(C–N–H)], 856.5 [$\delta_{out\ pl.}$ (C–C–H)$_{mes}$], 736.2, 666.6 cm^{-1} [$\delta_{out\ pl.}$ (C–C–H)$_{pyr}$].

$\{(C_5H_6N)_3[(mesTeI_3)(\mu\text{-}I^-)(TeI_3mes)](I_3)_2\}_n$ (**3**): hygroscopic, rectangular black crystals. $C_{33}H_{40}I_{13}N_3Te_2$ (2383.58). Yield: 88.0% based on $(mesTe)_2$; Melting point: 143.8–145.5 °C. C, H, N-analysis, Found: C, 15.75; H, 1.95; N, 2.05. Calc.: C, 16.63; H, 1.69; N, 1.76%.

IR (KBr): 3215.0 [ν(N–H)], 3152.4 [ν(C–H)$_{ar}$], 3057.2 [ν(C–H)$_{me}$], 1627.7 [ν(C=C)], 1595.0 [ν(C=N)], 1524.1 [δ(C–C–H)], 1475.7 [δ(C–N–H)], 837.4 [$\delta_{out\ pl.}$ (C–C–H)$_{mes}$], 726.5, 662.3 cm^{-1} [$\delta_{out\ pl.}$ (C–C–H)$_{pyr}$].

2.3. Crystallography

Single crystals fixed on a glass fiber were used for the X-ray data collection. Data were collected with a Bruker APEX II CCD area-detector diffractometer and graphite-monochromatized Mo Kα radiation. Computing data reduction and absorption correction [8]. The structures of $[mesTeI(\mu\text{-}I)_2(TeImes)_2]_n$ (**1**), $(C_5H_6N)_4[mesTeI_2]_2$ $(I_3)_2$ (**2**) and $\{(C_5H_6N)_3[(mesTeI_3)(\mu\text{-}I^-)(TeI_3mes)](I_3)_2\}_n$ (**3**) were solved by direct methods [9] and refined on F^2 with anisotropic temperature parameters for all non H atoms [10]. H atoms of the mesityl groups were positioned geometrically (C–H = 0.93 Å for Csp^2 atoms) and treated as riding on their respective C atoms, with U_{iso}(H) values set at $1.2U_{eq}Csp^2$. The hydrogen atom (N–H) of the pyridonium ion was located in a difference-Fourier map and refined isotropically. The crystallographic parameters and details of data collection and refinement are given in Table 1.

3. Results and discussion

Crystal data and experimental conditions are given in Table 1. Selected bond distances and angles of $[mesTeI(\mu\text{-}I)_2(TeImes)_2]_n$ (**1**), $(C_5H_6N)_4[mesTeI_2]_2$ $(I_3)_2$ (**2**) and $\{(C_5H_6N)_3[(mesTeI_3)(\mu\text{-}I^-)(TeI_3mes)]$ $(I_3)_2\}_n$ (**3**) are listed in Tables 2–4, with dashed lines representing the secondary bonds. Fig. 1 represents the unidimensional assembling of complex **1** in the *ab* plane; Fig. 2 shows the dimeric association of **2**. Fig. 3 displays the asymmetric unit of **3**, with the secondary interactions and charge delocalization in dashed

Table 1
Crystal data and structure refinement for **1**, **2** and **3**

	1	**2**	**3**
Empirical formula	$C_{27}H_{33}I_5Te_3$	$C_{19}H_{23}I_5N_2Te$	$C_{33}H_{40}I_{13}N_3Te_2$
Formula weight	1374.83	1041.49	2383.58
T (K)	293(2)	293(2)	293(2)
Radiation, λ (Å)	Mo Kα, 0.71	Mo Kα, 0.71	Mo Kα, 0.71
Crystal system	Monoclinic	Triclinic	Monoclinic
Space group	$P2_1/c$	$P\bar{1}$	$P2_1/c$
Unit cell dimensions			
a (Å)	8.1642(2)	8.4019(4)	16.2880(2)
b (Å)	28.5166(9)	8.6610(4)	17.4708(2)
c (Å)	16.0723(5)	21.2534(1)	21.1867(3)
α (°)	90	86.979(2)	90
β (°)	103.721(2)	89.221(2)	107.567(6)
γ (°)	90	63.966(1)	90
V (Å^3)	3635.09(18)	1387.65(12)	5747.82(12)
Z	4	2	4
Absorption coefficient (mm^{-1})	6.653	6.642	8.022
Crystal size (mm)	$0.06 \times 0.06 \times 0.23$	$0.07 \times 0.15 \times 0.25$	$0.10 \times 0.11 \times 0.43$
F (000)	2464	936	4208
θ Range (°)	1.43–28.33	0.96–30.59	1.31–30.14
Index ranges	$-10 \leqslant h \leqslant 8$, $-37 \leqslant k \leqslant 38$, $-21 \leqslant l \leqslant 18$	$-11 \leqslant h \leqslant 12$, $-12 \leqslant k \leqslant 12$, $-27 \leqslant l \leqslant 30$	$-22 \leqslant h \leqslant 22$, $-24 \leqslant k \leqslant 23$, $-29 \leqslant l \leqslant 29$
Reflections collected	25937	24062	122702
Reflections unique	8989 [$R_{int} = 0.0242$]	8493 [$R_{int} = 0.0208$]	16887 [$R_{int} = 0.0477$]
Absorption correction	Multi-scan (SADABS)	Multi-scan (SADABS)	Multi-scan (SADABS)
Maximum and minimum transmission	1.00 and 0.64	1.00 and 0.67	1.00 and 0.47
Refinement method	Full-matrix least-squares on F^2	Full-matrix least-squares on F^2	Full-matrix least-squares on F^2
Data/restraints/parameters	8989/0/316	8493/0/244	16887/0/460
Goodness-of-fit on F^2	1.093	1.023	1.135
Final R indices [$I > 2\sigma(I)$]	$R_1 = 0.0279$; $wR_2 = 0.0675$	$R_1 = 0.0403$; $wR_2 = 0.1362$	$R_1 = 0.0534$; $wR_2 = 0.1486$
R indices (all data)	$R_1 = 0.0418$; $wR_2 = 0.0807$	$R_1 = 0.0626$; $wR_2 = 0.1551$	$R_1 = 0.1204$; $wR_2 = 0.2028$
Largest difference in peak and hole (e Å^{-3})	0.985 and −0.812	1.226 and −2.239	2.382 and −1.997

Table 2
Selected bond lengths [Å] and angles [°] for $[mesTeI(\mu\text{-}I)_2(TeImes)_2]_n$ (**1**)

Bond lengths		Bond angles	
C(11)–Te(1)	2.139(0)	I(1)–Te(1)–I(2)	172.85(2)
Te(1)–I(1)	2.794(7)	I(2)–Te(3)–I(5)	173.48(0)
Te(1)–I(2)	3.148(7)	Te(1)–I(2)–Te(3)	99.94 (1)
Te(1)–I(3)	2.924(6)	Te(1)–I(2)–Te(2)′	101.51(0)
C(21)–Te(2)	2.121(0)	Te(1)–I(3)–Te(2)	172.52(2)
Te(2)–I(3)	3.063(7)	I(4)–Te(2)–I(2)″	175.33(1)
Te(2)–I(4)	2.752(7)	C(11)–Te(1)–I(1)	90.73(1)
Te(2)′–I(2)	3.297(0)	C(11)–Te(1)–I(2)	84.84(1)
C(31)–Te(3)	2.130(6)	C(11)–Te(1)–I(3)	113.44(1)
Te(3)–I(2)	3.340(0)	C(21)–Te(2)–I(3)	116.33(1)
Te(3)–I(5)	2.751(8)	C(21)–Te(2)–I(4)	94.04(1)
		C(31)–Te(3)–I(2)	82.49(1)
		C(31)–Te(3)–I(5)	91.64(1)

Symmetry transformations used to generate equivalent atoms: (′) = −1 + x, y, z; (″) = 1 + x, y, z.

lines. Fig. 4 exhibits the polymerization of **3** in the *ab* plane. In the polymeric assembling of $[mesTeI(\mu\text{-}I)_2(TeImes)_2]_n$ (**1**, Fig. 1) the I(2) atom attains a triple bridge function, linking Te(1) {Te(1)–I(2) = 3.148(7)}, Te(2) {Te(2)′–I(2) = 3.297(0)} and T(3) {Te(3)–I(2) = 3.340(0) Å}. The μ_2-I(3) distances I(3)–Te(1) and I(3)–Te(2) are 2.924(6) and 3.063(7) Å respectively. The Te(3)–I(2) {3.340(0)} and Te(3)–I(5) {2.751(8) Å} distances show that $[mesTeI(\mu\text{-}I)_2(TeImes)_2]_n$ (**1**) formally can be viewed as Te^{IV} moieties {Te(1) and Te(2)} linked to Te^{II} groups {Te(3)}, e.g., the tellurium atoms attain mixed valence states in the same molecule, a very rare occurrence form of organochalcogen halides [11,12]. In addition, such clear molecular association between $[mesTeI_3]$ and [mesTeI] moieties has not yet been reported in the solid state.

The complex salt $(C_5H_6N)_4[mesTeI_2]_2\ (I_3)_2$ (**2**) exhibits atypical secondary interactions – through iodine atoms – between the *anions* I_3^- and $[mesTeI_2]^-$. These twofold negatively charged units are combined in dimers through reciprocal Te(1)···I(1) interactions {3.924(3) Å}, with the I(1)/I(1)′ and (I2)/(I2)′ atoms fulfilling the charge balance

Table 3
Selected bond lengths [Å] and angles [°] for $(C_5H_6N)_4[mesTeI_2]_2(I_3)_2$ (**2**)

Bond lengths		Bond angles	
C(11)–Te(1)	2.130(5)	C(11)–Te(1)–I(1)	89.14(1)
Te(1)–I(1)	2.919(6)	C(11)–Te(1)–I(2)	89.81(1)
Te(1)–I(2)	2.974(6)	I(1)–Te(1)–I(2)	178.90(2)
I(2)···I(3)	3.659(4)	Te(1)–I(2)···I(3)	146.86(2)
I(3)–I(4)	2.896(8)	I(3)–I(4)–I(5)	179.45 (2)
I(4)–I(5)	3.006(8)	I(1)···H(31)′–N(31)′	133.82(1
Te(1)···I(1)′	3.924(3)	I(2)···H(21)–N(21)	144.80(2)
I(1)···H(31)′	3.158(2)		
I(2)···H(21)	2.904(2)		

Symmetry transformations used to generate equivalent atoms: (′) = −x, 1 − y, −z.

Table 4
Selected bond lengths [Å] and angles [°] for $\{(C_5H_6N)_3[(mesTeI_3)(\mu\text{-}I)(TeI_3mes)](I_3)_2\}_n$ (**3**)

Bond lengths		Bond angles	
C(11)–Te(1)	2.147(8)	C(11)–Te(1)–I(1)	89.2(2)
Te(1)–I(1)	2.884(10)	C(11)–Te(1)–I(2)	91.2(2)
Te(1)–I(2)	2.956(10)	C(11)–Te(1)–I(3)	116.2(2)
I(1)···I(8)	3.675(12)	C(11)–Te(1)···I(5)″	156.59(1)
I(8)–I(9)	2.856(11)	I(1)···I(8)–I(9)	167.12(2)
I(9)–I(10)	2.982(12)	Te(1)–I(3)–I(4)	172.53(3)
Te(1)–I(3)	2.826(9)	I(3)–I(4)–I(5)	95.87(3)
I(3)–I(4)	3.100(10)	C(21)–Te(2)–I(5)	116.9(2)
I(4)–I(5)	3.097(9)	C(21)–Te(2)–I(6)	89.1(2)
C(21)–Te(2)	2.149(4)	C(21)–Te(2)–I(7)	90.1(2)
Te(2)–I(5)	2.833(9)	C(21)–Te(2)···I(3)′	155.80(1)
Te(2)–I(6)	2.873(10)	Te(2)–I(5)–I(4)	171.77(3)
Te(2)–I(7)	2.974(11)	I(6)···I(11)–I(12)	165.48(1)
I(6)···I(11)	3.618(12)	N(31)–H(31)···I(13)	126.76(2)
I(11)–I(12)	2.865(12)	N(41)–H(41)···I(7)	133.04(2)
I(12)–I(13)	2.961(12)	N(51)–H(51)···I(10)	134.79(2)
Te(1)···I(5)″	3.922(7)	I(8)– I(9)–I(10)	179.20(1)
I(3)···Te(2)″	3.940(7)	I(11)–I(12)–I(13)	178.97(1)
H(31)···I(13)	3.279(6)		
H(41)···I(7)	3.150(2)		
H(51)···I(10)	3.265(6)		

Symmetry transformations used to generate equivalent atoms: (′) = $-x$, $0.5+y$, $0.5-z$; (″) = $-x$, $-0.5+y$, $0.5-z$.

by means of four N^+–H···I bonding {N–H(31)···I(1) = 3.158(2), N–H(21)···I(2) = 2.904(2) Å}, as shown in Fig. 2. The structure of $\{(C_5H_6N)_3(\mu\text{-}I^-)(TeI_3mes)]\ (I_3)_2\}_n$ (**3**) has also not yet been described. The complex asymmetric unit is assembled formally by the association of two mes-TeI_3 moieties through an iodide ion. The charge delocalization, also represented in Fig. 3, is suggested by the equivalence of the bond distances I(3)–I(4) {3.100(10)} and I(4)–I(5) {3.097(9) Å}. Also hier interanionic I_3^-···I–Te^- bonding and N^+–H···I–Te^- interactions take place, besides N^+–H···I_3^- effective contacts. The asymmetric units represented in Fig. 3 attain the complex polymeric, unidimensional structure shown in Fig. 4: each $(C_5H_6N)_3$-$(\mu\text{-}I^-)(TeI_3mes)](I_3)_2$ unit is linked to the half of two facing ones through reciprocal Te–I secondary interactions {Te(1)···I(5)″ = 3.922(7), Te(2)″···I(3) = 3.940(7) Å, see Fig. 4}, achieving a zigzag polymeric assembling of centrosymmetric dimers connected along the chain through iodine bridges. The presence, in **2** and **3**, of linear chains of I_3 anions {**2**: I(3)–I(4)–I(5) = 179.45(2)°; **3**: I(8)–I(9)–I(10) = 179.20(1)°, I(11)–I(12)–I(13) = 178.97(1)°} allows their classification as charge-transfer (CT) compounds, since the charge-transfer effect is associated with this anionic iodine species. Although we have not experimentally confirmed, in compound **3** a CT system probably is present also within the iodine atoms I(3), I(4) and I(5), as consequence (or perhaps as cause) of the charge delocalization.

Recently we have reported some new examples of simultaneous occurrence of secondary Te···I and I···I interactions: in the complex salts $(Et_4N)[PhTeI_4]$ and (Et_4N)-[(β-naphtyl)TeI_4] [13], only anionic interactions of the types Te···I and I···I take place, cation–anion effective contacts do not occur. For each case the secondary bonds keep the anionic moieties in a whole supramolecular gathering, being also able to assure an octahedral coordination to the tellurium atoms. The well known sequence of $[(\beta\text{-naphtyl})TeI_4]^-$ dimers – through reciprocal Te···I interactions – connected in chains by means of I···I bonding had been already found in the supramolecular lattice of (α-naphtyl)TeI_3 [14]. Further examples of interesting anion–anion and polymeric associations through Te···I and I···I interactions offer the lattices of $[p\text{-}CH_3O(C_6H_4)Te(etu)][p\text{-}CH_3O(C_6H_4)TeI_4]$ (etu = ethylenethiourea) and $[RTeI_3(\mu\text{-}I)Te(tu)R]$ {R = *p*-PhO-(C_6H_4); tu = thiourea}, recently described [15]. Typical "three center–four electron" bonds, i.e. triiodide like bonding involving Se···I and I···I interactions have also been shown by du Mont and co-workers [16] in solid $\{[C_5H_{10}N_2\text{–}Se]_2^{2+} \cdot 2I_3^- \cdot C_5H_{10}N_2\text{–}Se - I_2\}$.

It is well known that the heavier halogens, particularly I_2, tend to form oligomeric catenated polyanions which can assume a wide range of structural designs [17]. Polyiodides such as I_3^-, I_4^{2-} and I_5^- are very numerous in the literature and have been well discussed by Devillanova, Lippolis

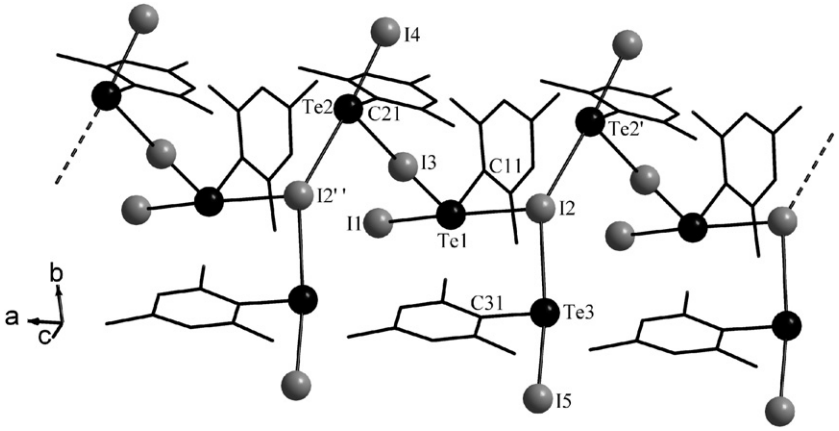

Fig. 1. Unidimensional assembling of $[mesTeI(\mu\text{-}I)_2(TeImes)_2]_n$ (**1**) in the *ab* plane. Symmetry transformations used to generate equivalent atoms: (′) = $-1+x$, y, z; (″) = $1+x$, y, z.

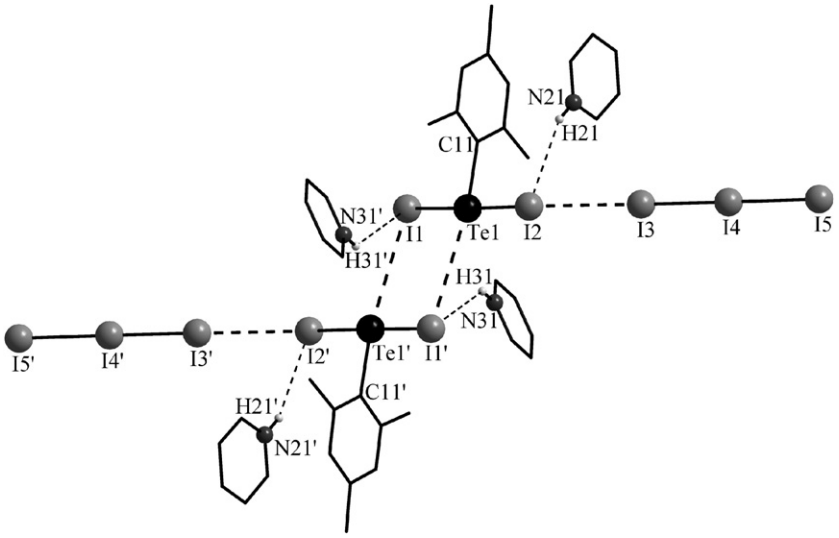

Fig. 2. Structure of the dimer $(C_5H_6N)_4[mesTeI_2]_2(I_3)_2$(**2**). Symmetry transformations used to generate equivalent atoms: $(') = -x, 1 - y, -z$. Dashed lines are secondary interactions.

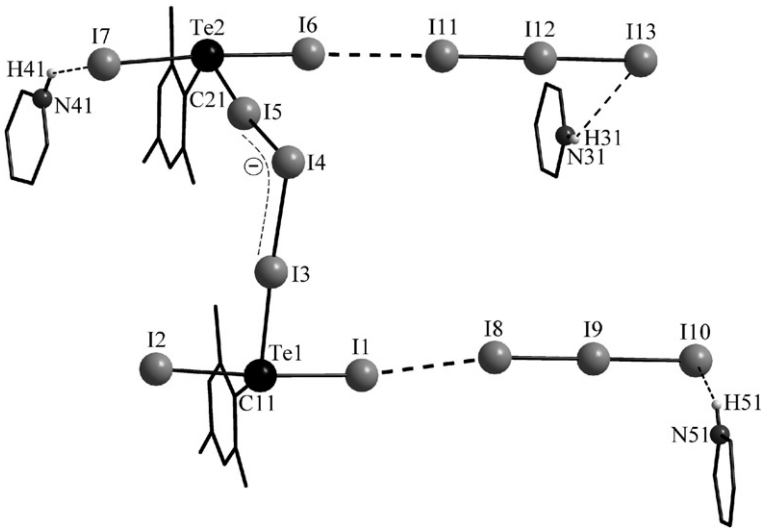

Fig. 3. Asymmetric unit of $\{(C_5H_6N)_3[(mesTeI_3)(\mu\text{-}I^-)(TeI_3mes)](I_3)_2\}_n$. Dashed lines represent secondary bonding and charge delocalization.

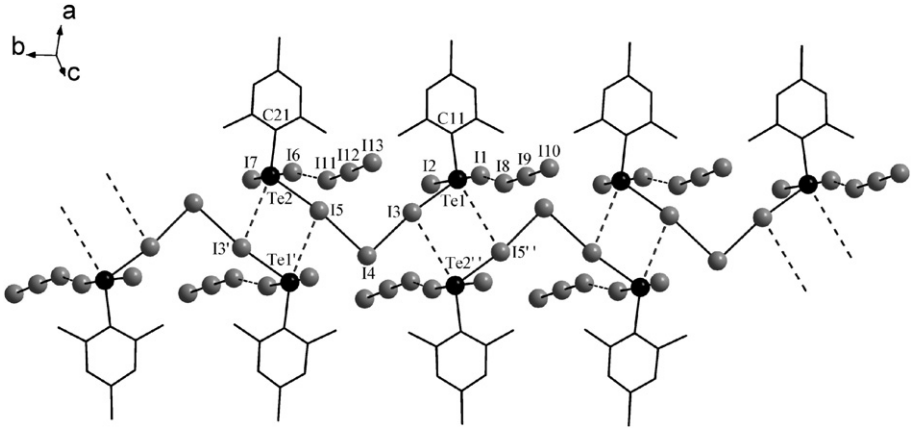

Fig. 4. Polymerization of $\{(C_5H_6N)_3[(mesTeI_3)(\mu\text{-}I^-)(TeI_3mes)](I_3)_2\}_n$ in the *ab* plane, with dashed lines representing secondary interactions. For clarity the pyridinium cations do not appear. Symmetry transformations used to generate equivalent atoms: $(') = -x, 0.5 + y, 0.5 - z$; $('') = -x, -0.5 + y, 0.5 - z$.

and co-workers [18], according to whom all higher polyiodides can be considered to be derived from the donor/acceptor interaction of asymmetric I_3^- and/or I^- with di-iodine molecules that emerge slightly elongated. Although some polyiodides are present in the crystal lattices as discrete aggregates, they frequently attain polymeric one-dimensional chains or extended two- or three-dimensional networks in the polyanionic matrix via I···I cross-linking soft–soft secondary interactions: these range generally from 3.6 Å up to the van der Waals sum for two iodine atoms (4.3 Å) [19], and the identification of the basic polyiodide unit can become arbitrary [17,20]. However, the value of 3.6 Å for an I···I is commonly accepted as the borderline for the identification of the basic polyiodide unit in extended multi-dimensional polyanionic networks [17]: values lower than 3.6 Å identify the polyiodide unit, values higher than this limit distance should be considered as contacts between polyiodide units.

Although our results do not deal with higher polyiodide chains, all the measured values for I–I bond distances in the complexes **2** and **3** (see Tables 3 and 4) are limited by 3.6 Å: lower values identify covalent I–I bonds, longer distances characterize the secondary I–I interactions between single I_3^- and I–$Te^{\ominus}$–I chains. Finally, is has been also pointed out [18] that bond angles of iodine chains are frequently observed at 90° and 180°, but can deviate considerably from these values with longer (I_3^-) I^-···I–I bond lengths.

4. Supplementary material

CCDC 619645, 619646 and 619647 contains the supplementary crystallographic data for **1**, **2** and **3**. These data can be obtained free of charge via http://www.ccdc.cam.ac.uk/conts/retrieving.html, or from the Cambridge Crystallographic Data Centre, 12 Union Road, Cambridge CB2 1EZ, UK; fax: (+44) 1223-336-033; or e-mail: deposit@ccdc.cam.ac.uk.

References

[1] G. Manzoni de Oliveira, E. Faoro, E. Schulz Lang, G.A. Casagrande, Z. Anorg. Allg. Chem. 632 (2006) 659.
[2] E. Schulz Lang, G. Manzoni de Oliveira, G. Antonio Casagrande, J. Organomet. Chem. 691 (2006) 59.
[3] E. Faoro, G. Manzoni de Oliveira, E. Schulz Lang, Z. Anorg. Allg. Chem. 632 (2006) 2049.
[4] L.-O. Klotz, K.-D. Kröncke, D.P. Buchczyk, H. Sies, J. Nutr. 133 (2003) 1448S.
[5] M.A. Lucas, O.T.K. Nguyen, C.H. Schiesser, S.-L. Zheng, Tetrahedron 56 (2000) 3995.
[6] N. Al-Maharik, L. Engman, J. Malmström, C.H. Schiesser, J. Org. Chem. 66 (2001) 6286.
[7] Radioisotopes in Medicine, Nuclear Issues Briefing Paper 26, Published by Uranium Information Centre Ltd. GPO Box 1649N, Melbourne 3001, Australia, phone (03) 9629 7744.
[8] SADABS: N. Walker, D. Stuart, Acta Crystallogr A39 (1983) 158.
[9] M.C. Burla, R. Caliandro, M. Camalli, B. Carrozzini, G.L. Cascarano, L. De Caro, C. Giacovazzo, G. Polidori, R. Spagna, J. Appl. Cryst. 38 (2005) 381.
[10] G.M. Sheldrick, SHELXL-97, Program for Crystal Structure Refinement, University of Göttingen, Germany, 1997.
[11] H.M.K.K. Pathirana, J.H. Reibenspies, E.A. Meyers, R.A. Zingaro, Acta Cryst. C47 (1991) 516.
[12] E. Schulz Lang, G.A. Casagrande, G. Manzoni de Oliveira, G.N. Ledesma, S.S. Lemos, E.E. Castellano, U. Abram, Eur. J. Inorg. Chem. 5 (2006) 958.
[13] E. Schulz Lang, G. Manzoni de Oliveira, G.N. Ledesma, Z. Anorg. Allg. Chem. 631 (2005) 1524.
[14] E. Schulz Lang, G. Manzoni de Oliveira, E.T. Silveira, R.A. Burrow, E.M. Vázquez-López, J. Organomet. Chem. 664 (2002) 306.
[15] G.A. Casagrande, E. Schulz Lang, G. Manzoni de Oliveira, S.S. Lemos, V.A.S. Falcomer, J. Organomet. Chem. 691 (2006) 4006.
[16] W.-W. du Mont, A. Martens-von Salzen, F. Ruthe, E. Seppälä, G. Mugesh, F.A. Devillanova, V. Lippolis, N. Kuhn, J. Organomet. Chem. 623 (2001) 14.
[17] P.H. Svenson, L. Kloo, Chem. Rev. 103 (2003) 1649, and references therein.
[18] M.C. Aragoni, M. Arca, F. Demartin, F.A. Devillanova, A. Garau, F. Isaia, V. Lippolis, S. Rizzato, G. Verani, Inorg. Chim. Acta 357 (2004) 3803.
[19] S.C. Nyburg, C.H. Faerman, Acta Crystallogr. B 41 (1985) 274; D. Kirin, Acta Crystallogr. B 43 (1987) 274.
[20] A.J. Blake, F.A. Devillanova, R.O. Gould, W.-S. Li, V. Lippolis, S. Parsons, C. Radek, M. Schröder, Chem. Soc. Rev. 27 (1998) 195.